IVYSPRING INTERNATIONAL PUBLISHER

Theranostics

2016; 6(12): 2209-2224. doi: 10.7150/thno.15584

Research Paper

Lycorine Downregulates HMGB1 to Inhibit Autophagy and Enhances Bortezomib Activity in Multiple Myeloma

Mridul Roy[1*], Long Liang[1*], Xiaojuan Xiao[1*], Yuanliang Peng[1*], Yuhao Luo[1], Weihua Zhou[1], Ji Zhang[1], Lugui Qiu[2], Shuaishuai Zhang[2], Feng Liu[3], Mao Ye[4]✉, Wen Zhou[5]✉, Jing Liu[1]✉

1. The State Key Laboratory of Medical Genetics & School of Life Sciences, Central South University, Changsha 410078, China.
2. Key Laboratory of Experimental Hematology, Institute of Hematology & Blood Diseases Hospital, Chinese Academy of Medical Science & Peking Union Medical College, Tianjin 300020, China.
3. Department of Medicine, University of California, Irvine, CA 92697, USA.
4. Molecular Science and Biomedicine Laboratory, State Key Laboratory for Chemo/Biosensing and Chemometrics; College of Biology; College of Chemistry and Chemical Engineering, Hunan University, Changsha 410082, China.
5. Cancer Research Institute, Central South University; Key Laboratory of Carcinogenesis and Cancer Invasion, Ministry of Education; Key Laboratory of Carcinogenesis, National Health and Family Planning Commission, Changsha 410078, China.

*These authors contributed equally to this work.

✉ Corresponding authors: Jing Liu, e-mail address: jingliucsu@hotmail.com or liujing2@sklmg.edu.cn; Tel: +86-731-84805026, Fax: +86-731-84805026; Wen Zhou, e-mail address: zw20042@126.com; Mao Ye, e-mail address: goldleaf@hnu.edu.cn.

Received: 2016.03.19; Accepted: 2016.08.12; Published: 2016.09.24

Abstract

Multiple myeloma (MM) is largely incurable and drug-resistant. Novel therapeutic approaches such as inhibiting autophagy or rational drug combinations are aimed to overcome this issue. In this study, we found that lycorine exhibits a promising anti-proliferative activity against MM in vitro and in vivo by inhibiting autophagy. We identified High mobility group box 1 (HMGB1), an important regulator of autophagy, as the most aberrantly expressed protein after lycorine treatment and as a critical mediator of lycorine activity. Gene expression profiling (GEP) analysis showed that higher expression of HMGB1 is linked with the poor prognosis of MM. This correlation was further confirmed in human bone marrow $CD138^+$ primary myeloma cells and MM cell lines. Mechanistically, proteasomal degradation of HMGB1 by lycorine inhibits the activation of MEK-ERK thereby decreases phosphorylation of Bcl-2 resulting in constitutive association of Bcl-2 with Beclin-1. In addition, we observed higher HMGB1 expression in bortezomib resistant cells and the combination of bortezomib plus lycorine was highly efficient in vitro and in vivo myeloma models as well as in re-sensitizing resistant cells to bortezomib. These observations indicate lycorine as an effective autophagy inhibitor and reveal that lycorine alone or in combination with bortezomib is a potential therapeutic strategy.

Key words: Lycorine; Multiple myeloma; Autophagy; HMGB1; Bortezomib resistance.

Introduction

Multiple myeloma (MM) is the second most prevalent hematologic malignancy, characterized by the infiltration of malignant plasma cells into bone marrow. In spite of current efficient therapeutic regimens for MM patients, such as the proteasome inhibitor bortezomib, which has marked efficacy against MM, the major features inevitably present in this disease are the intrinsic and acquired resistance to bortezomib [1, 2]. There is an urgent need in clinic for understanding the genetic makeup of these drug-resistant myeloma cells so that novel agents can be developed to treat MM patients [3, 4].

Autophagy removes defective cellular organelles, protein aggregates, and intracellular microbes and is associated with cell survival, thereby beneficial for tumor maintenance [5, 6]. Studies demonstrated that inhibition of autophagy enhances sensitivity of a number of anticancer agents and induces cell death in MM [7-11]. Currently, clinically relevant autophagic inhibitors being used for cancer

therapy are chloroquine, hydroxychloroquine and lucanthone and novel inhibitors with a lower toxicity and a better therapeutic index are in demand [12]. High-mobility group box-1 (HMGB1) protein is an important autophagy modulator. In the regulation of autophagy HMGB1 plays subcellular localization-dependent roles [13-15]. Since the identification in 1973, HMGB1 has been implicated in several disease states including cancer [16, 17]. Although the link between HMGB1 and MM has not been clarified previously, the importance of HMGB1 for induction of autophagy and tumor development has made this protein as a novel target for cancer therapy [15, 18-20].

Owing to their availability in nature and therapeutic compatibility, many natural compounds have been investigated for their anti-cancer properties over decades and several of these compounds have been increasingly integrated into modern medicine [21, 22]. Vinca alkaloids, vinblastine (VLB) and vincristine (VCR) were the first approved natural anti-cancer drugs, and currently over 60% of commercially available anticancer drugs are of natural origin [23, 24]. Therefore, exploring the biological activity and identifying the efficient interacting molecules of these natural anti-cancer compounds has become an indispensible element for novel drug discovery.

Lycorine is a natural compound obtained from the Amaryllidaceae plant family. In 2004, our group found the first evidence that lycorine exhibits activities against leukemia [25, 26]. Later observations demonstrated the anti-proliferative effects of lycorine in other hematological malignancies and several other solid tumors [27-31]. Although previous studies mainly showed lycorine as a potential apoptosis inducer, a recent study, based on the chemical structure, stated that apoptosis is not the primary mechanism for anti-proliferative activity of this compound [32]. This led the interest to investigate the role of lycorine on other cell maintenance systems, such as autophagy. In addition, single-agent efficacy of lycorine or in combination with other anti-MM agents has not been evaluated in vivo MM models.

In this study, we explored the effect of lycorine on MM cells, in MM xenograft mouse and on primary myeloma patient samples, and the role of this natural agent on regulation of autophagy in vitro and in vivo. Furthermore, lycorine treatment was combined with bortezomib (BTZ), with or without bone marrow stromal cells (BMSCs) and MM xenograft mouse model, to investigate potential clinical application of lycorine in treating MM.

Materials and methods

Chemicals and antibodies

Lycorine (Sigma, MO, USA) was dissolved in dimethylsulfoxide (DMSO) (Sigma) and stored at -20°C. 3-MA and MG-132 was obtained from Selleckchem (TX, USA). Cell Counting Kit-8 (CCK8) was obtained from Vazyme Biotech Co., (Nanjing, China). Antibodies used were LC3B, Beclin-1, Ubiquitin, MEK (Cell Signaling Technology, MA, USA), HMGB1 (Abcam, MA, USA), Bcl-2, p-Bcl-2, MEK, p-MEK, ERK1/2, p-ERK1/2, RCC1, α-Tubulin and GAPDH (Santa Cruz Biotechnology, TX, USA).

Cell culture and treatment

ARP-1 and ANBL6 cell lines were obtained from Institute of Hematology & Blood Diseases Hospital, Chinese Academy of Medical Science & Peking Union Medical College, Tianjin, China. ARH-77, MM.1S, and NCI-H929 (H929) cell lines were obtained from the American Type Culture Collection (ATCC, USA). Human peripheral B lymphocytes (B-cells) were obtained from the State Key Laboratory of Medical Genetics. All cell lines were cultured in RPMI 1640 medium (Gibco, MA, USA) supplemented with 10% fetal bovine serum (FBS) (Gibco), 100 U/ml penicillin and 100 μg/ml streptomycin (Thermo Fisher Scientific, MA, USA) in 5% CO_2 at 37°C. For B-cells and primary human $CD138^+$ cells, 15% FBS was used with complete growth medium. Cells were treated for 24 h with lycorine or/and Bortezomib (BTZ) diluted to various concentrations in serum-free medium. Amino acid starvation condition was induced by Hank's balanced salt solution (HBSS) supplemented with glucose.

Patient samples and primary human $CD138^+$ cell isolation

The study involving human patient samples and animal models were performed in accordance with the ethical standards of the Central South University Institutional Review Board Committee on human experimentation and animal care and used committee approved procedures.

Bone marrow aspirates were obtained from patients with myeloma and subjects who underwent bone marrow aspirate procedure for other disease were found to have normal plasma cells. Primary human $CD138^+$ cells were isolated from the bone marrow aspirates of these subjects by human CD138 enrichment kit ($CD138^+$ Plasma Cell Iso. Kit, Miltenyi Biotech, Bergisch Gladbach, Germany).

Cell viability, cell proliferation and cell apoptosis assay

Cell viability was measured using a Cell Counting Assay Kit (CCK)-8 according to manufacturer's protocol. Absorbance was measured at 450 nM using a microplate reader (Randox Toxicology, Crumlin, UK). Cell proliferation was counted manually using the trypan blue exclusion assay. Apoptotic cells were quantified using a FACSCalibur (BD Biosciences) flow cytometer after staining with Annexin V-FITC/PI staining kit (BD Biosciences, NJ, USA).

2-DE and MALDI-TOF/TOF-MS

Approximately 1000 µg of each protein sample from the whole-cell lysate was rehydrated with DeStreak Rehydration Solution (GE Healthcare, Amersham, UK) according to the manufacturer's instructions and applied to immobilized pH gradient (IPG) strips (GE Healthcare). The IPGphor system was programmed according to standard procedure. Each sample was run on 2-D gels at 16 mA for 15 min and then at 32 mA for approximately 5 h. After 2-DE, Coomassie brilliant blue G-250 (Bio-Rad, CA, USA) was used to visualize the protein spots in the 2-D gels. The gels were scanned using a UMAX PowerLook III scanner (UMAX) and analyzed using ImageMaster 2D Platinum software (GE healthcare). Proteins with at least a 2-fold differential expression were identified by MALDI-TOF/TOF-MS. Both the MS and MS/MS data were analyzed using GPS Explorer software-V3.6 (Applied Biosystems, MA, USA). The resulting peak list files were submitted to http://www.matrixscience.com using the Mascot search engine to identify the proteins in the MS/MS ion search pattern. The following parameters were considered: SwissProt 2015_11 (549832 sequences), *Homo sapiens* (human) taxonomy (20194 sequences), digestion enzyme trypsin, one missed cleavage site, fixed carbamidomethylated cysteine modification and partial oxidized methionine modification. The MS tolerance was set to 100 ppm, and the MS/MS tolerance was set to 0.3 Da. Known contaminant ions (keratin) were excluded. A Mascot MS/MS total ion score of greater than 56 was considered statistically significant ($p<0.05$).

Plasmid construction, shRNA and transient transfection

Human HMGB1 coding sequence was amplified from human cDNA by PCR using Platinum Taq DNA polymerase high fidelity (Thermo Fisher Scientific) and cloned into pCMV-tag2B vectors by the ClonExpress II One Step Cloning Kit (Vazyme Biotech Co.). The primer pairs for the pCMV-tag2B vector: 5′-TCCCCCGGGCTGCAGGAATTCATGGGCAAAG GAGATCCTAAG and 5′-GTCGACGGTATCGATAA GCTTTTATTCATCATCATCATCTTCTTC (Sangon Biotech, Shanghai, China). pcDNA3.1-green fluorescent protein-light-chain 3 (LC3-GFP) plasmids were purchased from Yingrun Biological Technology Co., China. Validated shRNA for HMGB1 was purchased from (Sigma). LC3-GFP and control plasmids, Control pCMV, HMGB1-pCMV, shHMGB1 and scramble shRNA were transfected using LipoMax reagent (Sudgen Biotechnology Inc, Ltd. WA, USA) according to manufacturer's protocol.

Transmission electron microscopy (TEM)

Cells were fixed with 2.5% glutaraldehyde for 24 h, post-fixed with 2% OsO4 for 2 h, followed by dehydration. Thin sections (50 nm) were cut on an Ultramicrotome (LKB-3 microtome, Sweden) and stained with uranyl acetate and lead citrate. Images were visualized by transmission electron microscope (HT7700, Japan).

Protein extraction and Western blotting

Whole cell lysates were prepared using RIPA buffer (Thermo Fisher Scientific) in the presence of a protease inhibitor and PhosStop (Roche, Basel, Switzerland). Cytoplasmic and nuclear proteins were isolated using a ProteoJET Cytoplasmic and Nuclear Protein Extraction Kit (Thermo Fisher Scientific). Protein from cultured medium was isolated by evaporating the medium. The protein concentration was quantified using a Pierce Bicinchoninic Acid (BCA) Protein Assay Kit (Thermo Fisher Scientific). Equal amounts of protein were blotted, and the blots were incubated with a primary antibody, followed by HRP conjugated to a suitable secondary antibody. Blots were developed using the SuperSignal West Pico Substrate (Thermo Fisher Scientific) chemiluminescence kit and Gene Genius Bio-imaging System (Bio-Rad).

Quantitative RT-PCR.

RNA was extracted by TRIzol reagent (Life technologies, CA, USA) using standard procedure. Primers used for RT-PCR were for HMGB1 (forward 5′ GGGCAAAGGAGATCCTAAGAAG 3′; reverse 5′GTTGACTGAAGCATCTGGGT3′) and GAPDH (forward 5′CATGAGAAGTATGACAACAGCCT3′; reverse 5′AGTCCTTCCACGATACCAAAGT3′) (Sangon Biotech.).

Cycloheximide (CHX) pulse-chase assay for protein stability

Cells treated with or without lycorine were chased in the presence of CHX (Solarbio, Beijing, China) for the indicated time periods. Cells harvested

at each time point were then processed for immunoblotting.

Co-IP reactions

Whole cell lysates were prepared for immunoprecipitation using IP lysis buffer (Beyotime, Wuhan, China). For each experiment, 500 µg of protein was incubated with 2 µg of primary antibody. After overnight incubation at 4°C, 20 µl of Dynabeads Protein G (Life Technologies) was added, and incubation was continued at 4 °C for 4 h. The beads were then washed with IP lysis buffer plus 0.1% Tween 20 (Life Technologies). Bound proteins were then eluted from the beads with 2× Laemmli sample buffer (BioRad) and analyzed by immunoblotting.

BMSCs and MM co-culture experiment

Bone marrow stromal cell (BMSC) line HS5 was obtained from ATCC and cultured in Dulbecco's Modified Eagle Medium (DMEM) (Gibco) supplemented with 10% fetal bovine serum, 100 units/ml penicillin, and 100 mg/ml streptomycin (Thermo Scientific) at 37°C and 5% CO_2. For co-culture, HS5 cells were seeded in 96-well plates and allowed to adhere. The next day, new medium containing suspended MM cells was added to the wells. Viability was measured using a CCK-8 assay after the treatment.

Gene Expression Profile (GEP) accession numbers

GEP database accession number for the microarrays performed on 44 subjects with MGUS, 12 subjects with SMM, and 559 newly diagnosed MM samples reported in this manuscript to analyze the expression of HMGB1 are GSE 5900 and GSE 2658.

Multiple myeloma xenograft mouse model

Non-obese diabetic/severe combined immunodeficiency (NOD/SCID) mice were irradiated with 200 cGy of γ radiation and, twenty-four hours later, the mice were subcutaneously inoculated in the flank with 5×10^6 MM.1S cells in 100 µl of phosphate-buffered saline (PBS). Mice were randomized into four groups when the tumors were measurable. The treatments included the intraperitonial injection of vehicle (control group), lycorine (5 mg/kg), BTZ (1 mg/kg) or lycorine plus BTZ (0.25mg/kg plus 1mg/kg). Mice were treated as presented in Supplementary Table S1. Tumor volume and body weight were checked every 4 days. Mice were euthanized after three consecutive treatment procedures. Tumors were processed for protein extraction or fixed with 10% formaldehyde and embedded in paraffin. Hematoxylin/eosin (HE) and TUNEL staining were performed according to standard protocols. Images were taken using an Olympus photomicroscope (Olympus, Japan) after mounting the stained slides.

Statistical analysis

Data are presented as the mean ± SD from at least three independent experiments. Differences were determined using a t-test and were considered statistically significant at $p<0.05$. For comparison among the different groups from GEP dataset, one way analysis of variance and Fisher's least significant difference test by SPSS 17.0 was used and the differences were considered statistically significant at $p<0.05$. Overall survival was measured using the Kaplan-Meier method, and the log-rank test was used for group comparison. Drug Synergy was quantified according to the Chou-Talalay Method for non-constant drug combination using the CalcuSyn software program (ComboSyn Inc., USA) [33]. A combination index (CI) <1.0 indicated synergistic effect, a CI=1 indicated additive effect, and a CI>1 indicated antagonistic effect.

Results

Lycorine decreases MM cell proliferation by inhibiting autophagy

To investigate the effect of lycorine on MM cell viability in vitro, 5 myeloma cell lines with different genetic backgrounds (ANBL6, ARP-1, ARH-77, H929, and MM.1S) and human immortal B lymphocytes (B-cells) were treated with increasing concentrations of lycorine for 24 h and the cell viability was analyzed. Lycorine significantly reduced the viability of MM cells ($p<0.01$) but did not significantly affect B-cells at the same concentrations ($p=0.837$, 0.061 and 0.141 for 2.5, 5, and 10 µM lycorine, respectively) (Figure 1A). Lycorine also induced apoptosis in MM cell regardless of genetic variation (Supplementary Figure S1). To check whether autophagy contributes to MM cell growth and whether autophagy inhibition contributes to lycorine anti-MM function, the autophagy inhibitor 3-Methyladenine (3-MA) was applied [34]. 3-MA treatment led to a significant decreased viability of both cell lines ($p<0.01$). This result confirmed previous finding that autophagy is beneficial for MM cell growth [35]. Surprisingly, combining 3-MA with lycorine did not obviously enhance the effect of lycorine when compared with lycorine single treatment (Figure 1B) suggesting the anti-proliferative mechanism of lycorine is associated with its effect of autophagy inhibition by sharing similar signaling pathway with that of phosphoinositide 3-kinase (PI3K) inhibitor 3-MA. Then the effect of lycorine on autophagy was

identified. The most important indicators of autophagy, LC3B and Beclin-1, were dramatically down regulated after lycorine treatment in different MM cell lines (Figure 1C). Transmission electron microscopy (TEM) showed significantly decreased (p<0.01) inhomogeneous vesicles in the cytoplasm of the ANBL6 and ARH-77 cell lines after treatment with lycorine compared with the control group (Figure 1D). Autophagy inhibition by lycorine was further confirmed under amino acid starvation condition. Starvation increased expression of LC3B and Beclin-1, and formation of punctuated aggregations of GFP-LC3 fluorescence in the cytoplasm. We found that lycorine inhibited starvation-induced LC3B level (Figure 1E) and the number of LC3 puncta in ANBL6 cells (Figure 1F). In comparison, treatment with autophagy inhibitor 3MA also showed decreased LC3B expression and LC3 puncta formation (Figure 1E and F). Together these finding suggested that lycorine inhibits autophagy as an anti-proliferative mechanism in MM.

HMGB1 acts as the key mediator of Lycorine induced autophagy inhibition

Autophagy is a fine tuned but complex cellular process. We next aimed to screen the protein(s) that are modulated by lycorine to inhibit autophagy. To this end 2-dimentional gel electrophoresis (2-DE) followed by matrix-assisted laser desorption ionization-time of flight mass spectrometry (MALDI-TOF/TOF-MS) was used after ARH-77 cells were treated for 24 h in presence or absence of lycorine. Among the protein characterized, HMGB1 was identified as the protein decreased to the highest extent after lycorine treatment (Figure 2A). HMGB1 was found to be decreased by lycorine treatment in a dose-dependent manner in ARH-77, ANBL6, ARP-1 and MM1.S cells, which confirmed the 2-DE results (Figure 2B). Given that HMGB1 is an important regulator of autophagy [13], we next evaluated the regulatory role of lycorine on HMGB1 and HMGB1 mediated autophagy. We performed gain-of- and loss-of-function analysis of HMGB1 by using pCMV-HMGB1 recombinant plasmid overexpression and HMGB1 shRNA mediated silencing system. Overexpression of HMGB1 in ARP-1 cells abrogated the anti-proliferative effect of lycorine (Figure 2C). In addition, we determined autophagy status in the absence or presence of lycorine in these cells. As anticipated, HMGB1 overexpression abolished lycorine-induced autophagy inhibition (Figure 2D). Contrary, specific reduction of HMGB1 expression upon transfection with shRNA ameliorated lycorine-induced cell viability in ARP-1 cells (Figure 2E). Knockdown of HMGB1 inhibited autophagy in absence of lycorine and the effect was significantly enhanced with lycorine treatment (Figure 2F). Together these data indicated that HMGB1 is required for autophagy induction and anti-myeloma action of lycorine is mediated via HMGB1 downregulation and subsequent repression of autophagy.

HMGB1 is overexpressed in MM and contributes to MM cell survival

To evaluate whether the expression of HMGB1 is linked with the prognosis of MM and the compatibility of targeting HMGB1 for MM treatment, we used the publicly available myeloma gene expression profiling (GEP) datasets GSE 5900 and GSE 2658. The result showed that the expression of HMGB1 was higher in 44 subjects with Monoclonal gammopathy of undetermined significance (MGUS), 12 subjects with Smoldering multiple myeloma (SMM), and 559 patients with newly diagnosed MM, in comparison to expression in 22 healthy subjects (Figure 3A). A Kaplan-Meier survival analysis was performed on the Total Therapy 2 and 3 (TT2 and 3) cohort from the GEP dataset to investigate the correlation between HMGB1 gene expression and overall survival (OS). Kaplan-Meier plot suggested natural cut-value between high and low-HMGB1 was determined by optimizing the correlation with survival. The optimal cut-value was determined at the median 12100 with hazard ratio, HR=1.736 including 95% confidence intervals. The correlation was significant at the investigated cut-off points with the top 50% of MM patients with highest HMGB1 expression showed a significantly lower OS (log-rank p=0.006) in the TT2 and TT3 treatment groups (Figure 3B). According to correlation analyses of clinical characteristics, HMGB1 gene expression represented an independent factor associated with poor prognosis in the TT2 and TT3 treatments. We also determined HMGB1 expression in primary human $CD138^+$ plasma cells isolated from the bone marrow aspirates of 9 healthy donors and 19 primary MM patients. Interestingly, HMGB1expression was increased in the $CD138^+$ cells in 27% (5 of 19) MM patients compared with healthy donors (p=0.040) (Figure 3C). Furthermore, we measured the expression level of HMGB1 protein in B-cell and 5 MM cell lines using Western blotting. HMGB1 expression was higher in almost all myeloma cell lines than that in the B-cell (Figure 3D). Moreover, we determined the role of HMGB1 in myeloma cell survival by silencing and overexpressing HMGB1 measuring cell viability and proliferation for different time period. Knockdown of HMGB1 induced efficiently greater inhibition of cell viability compared to control group (Figure 3E). We then investigated the effect of HMGB1 knockdown on

cell proliferation by using manual cell counting. We found that HMGB1 knockdown led to a decrease in cell proliferation (Figure 3F). In contrast, compared to mock-transfected group, HMGB1-transfected cells improved their viability with time (Figure 3G) and exhibited a faster cell growth trend compare to the control (Figure 3H). These data suggested that HMGB1 plays an important role in growth and proliferation of myeloma cells and provides a therapeutic rationale for targeting HMGB1 to treat MM.

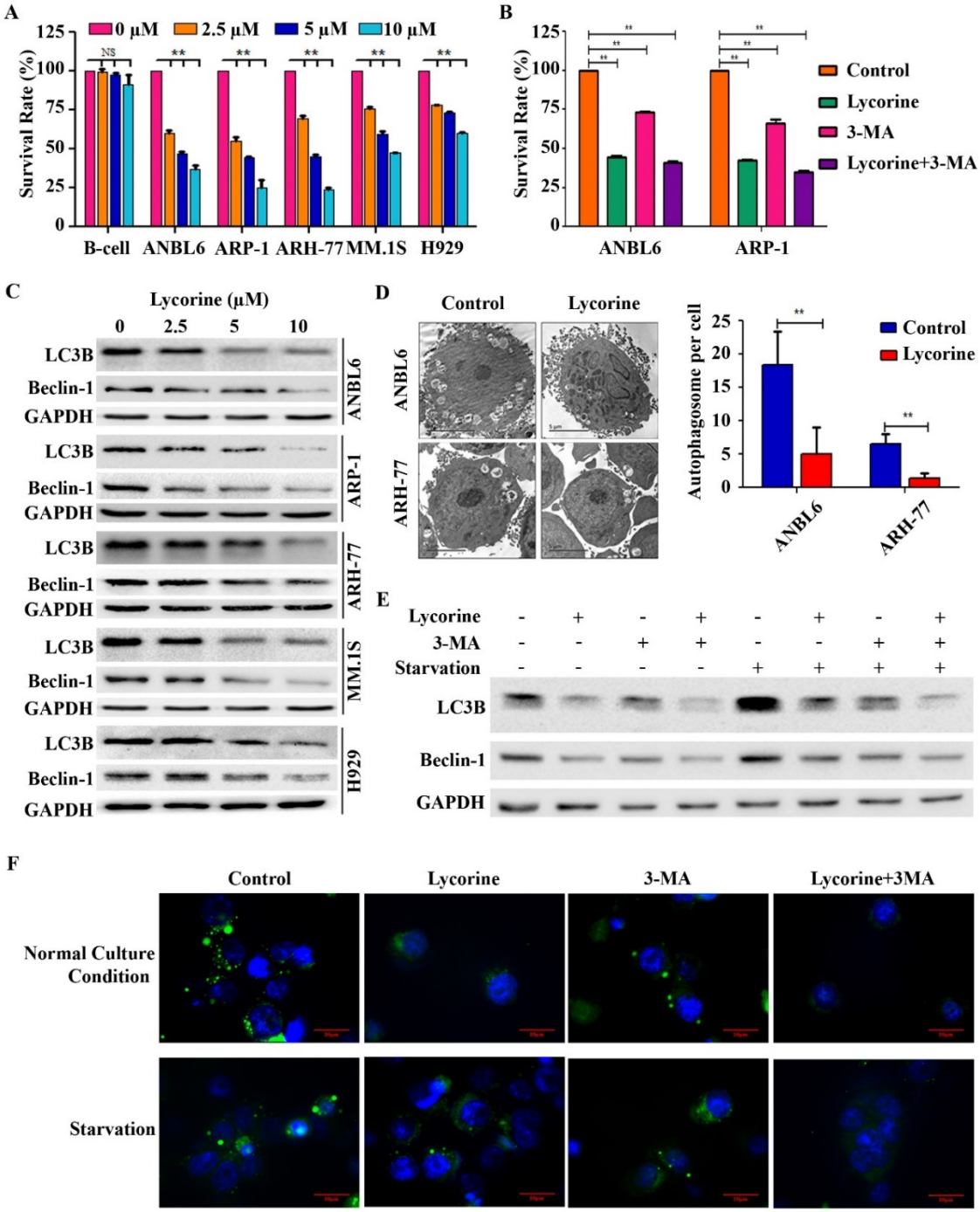

Figure 1. Lycorine decreases MM cell proliferation by inhibiting autophagy. (A) Effect of lycorine on cell viability. Different MM cell lines and a B-cell line were treated with the indicated concentrations of lycorine for 24 h. Cell survival rates were determined using a CCK-8 assay. The survival rate of 0 μM lycorine-treated cells was set to 100%. **(B)** Cells were treated with lycorine or/and the autophagy inhibitor 3-MA. Cell survival rates were analyzed using a CCK-8 assay. Data are representative of three independent experiments with mean±SD (***p*<0.01). **(C)** Expression of autophagy markers after lycorine treatment. Total protein was extracted and subjected to Western blotting using antibodies against the autophagy marker LC3B and Beclin-1. GAPDH was used as a loading control. **(D)** The morphological changes of lycorine treated ANBL6 and ARH-77 cells were detected by TEM. The number of autophagic vesicles per cells were counted from 35 randomly chosen cells and plotted on a graph (n=2, ***p*<0.01). **(E)** Lycorine blocks starvation-induced autophagy. ANBL6 cells were treated with starvation for 4 h with or without lycorine (10 μM) or 3-MA (10 μM) or both after a 20 h pre-treatment with or without lycorine. Cell extract was prepared and protein expression levels were assessed as indicated by Western blotting. **(F)** GFP-LC3B expression plasmid was transfected into ANBL6 cells. Transfected cells were treated as the conditions indicated in E and then were stained with Hoechst 33342. Autophagy was assayed by detecting the presence of GFP-LC3 punctae from three independent experiments using a fluorescence microscope (100×).

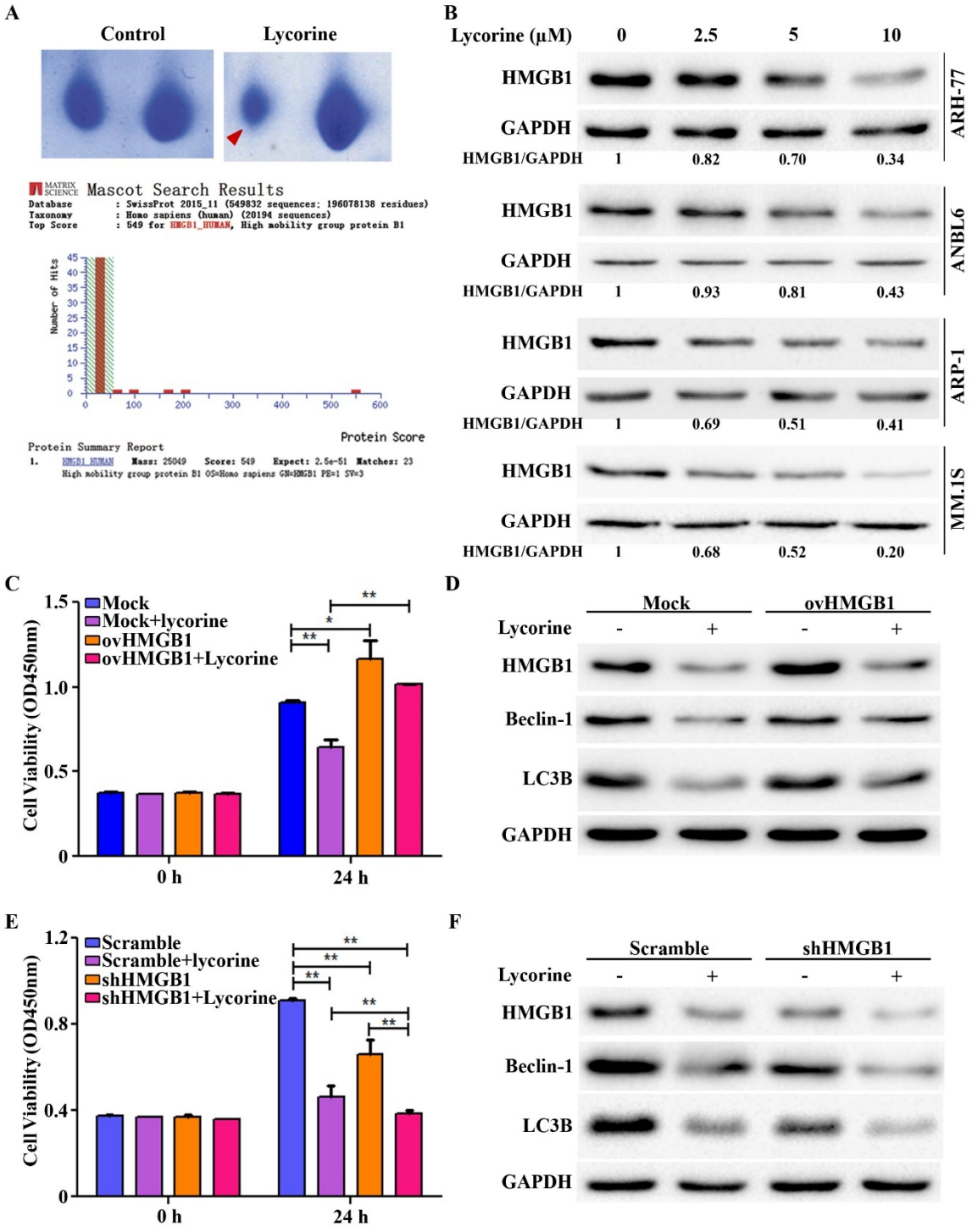

Figure 2. HMGB1 acts as the key mediator of lycorine induced autophagy inhibition. (A) Samples were prepared and separated by 2D gel electrophoresis to identify differentially expressed protein after lycorine treatment (5μM). The gel was stained with Coomassie blue and photographed. Section of the photograph is shown (top). The spot indicated by the red arrow in the top right panel corresponding to the most differentially expressed protein comparing the control (top left panel). HMGB1 was identified by the MASCOT search engine (bottom panel). The MASCOT search engine was used to assess the data from LC-MS/MS to identify the proteins from the UniProt protein database. HMGB1 had the highest hit score (549) among all possible hits contained in the database that matched the peptides from the sample. **(B)** ARH-77, ANBL6, ARP-1 and MM.1S cells were treated with indicated concentration of lycorine for 24 h and the expression of HMGB1 was analyzed in the cell extract by Western blotting. GAPDH was used as a loading control. The intensity of HMGB1 was determined by densitometry using ImageJ software and normalized with loading control (HMGB1/GAPDH). **(C)** ARP-1 cells were transfected with blank pCMV (Mock) or HMGB1-pCMV (ovHMGB1) vectors and cultured with or without lycorine for 24 h followed by cell viability analysis using a CCK-8 kit. Data are presented from three independent experiments. **(D)** ARP-1 cells transfected with blank or HMGB1 vectors were treated with or without lycorine and Western blotting was used to investigate the change in autophagy. GAPDH was used as a loading control. **(E)** ARP-1 cells were transfected with HMGB1 shRNA or scramble shRNA and cultured in the presence or absence of lycorine for 24 h and cell viability was measure using a CCK-8 kit. Data presented are mean±SD from three independent experiments. **(F)** Scramble or HMGB1 shRNA transfected ARP-1 cells were cultured for 24 h in the presence or absence of lycorine, the whole cell lysate was prepared and subjected to immunoblotting to detect autophagy. GAPDH was used as an internal control.

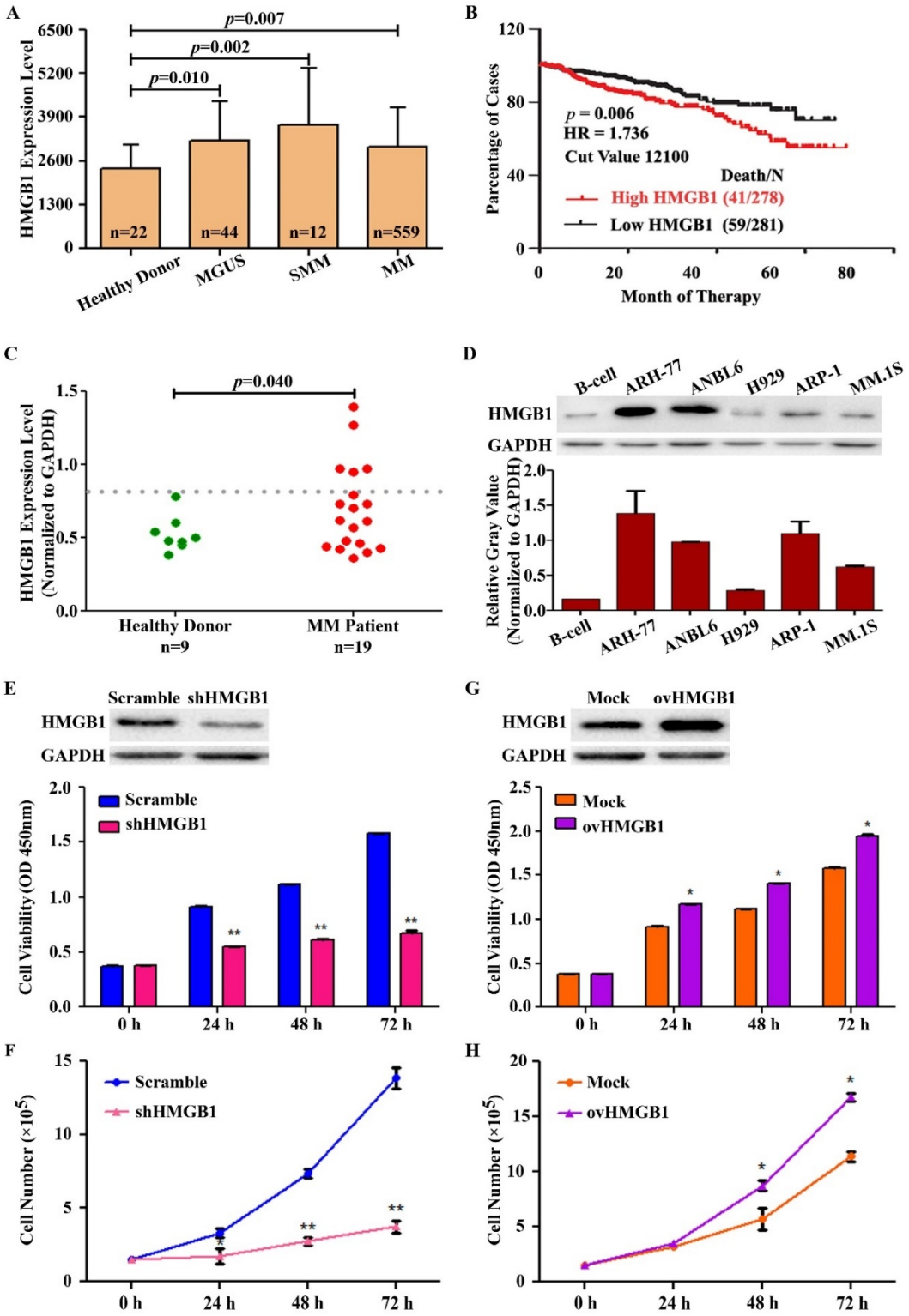

Figure 3. HMGB1 is overexpressed in MM and contributes to MM cell survival. (A) The expression of HMGB1 from microarray analysis of samples obtained from healthy donors and from MGUS, SMM and MM patients. Data presented as the mean±SD. **(B)** Kaplan-Meier analyses of overall survival (OS). Publicly available microarray data sets GSE 5900 and GSE 2658 were downloaded and data were reproduced to estimate the OS. **(C)** Expression of HMGB1 mRNA in primary human BM CD138$^+$ cell. Primary human CD138$^+$ cells were isolated from the BM aspirates of normal subjects (n=9) and patient with myeloma (n=19). GAPDH normalized HMGB1 mRNA level was analyzed by quantitative RT-PCR. **(D)** HMGB1 expression in myeloma cell lines and B-cell was measured by Western blotting. GAPDH was used as a loading control. Densitometry analysis of HMGB1 intensity was performed using ImageJ software, normalized with loading control (HMGB1/GAPDH) and plotted on a bar diagram. **(E)** A CCK-8 assay was used to check cell viability after ARP-1 cells were transiently transfected with HMGB1 shRNA or scramble shRNA for various times. Data are presented as the mean±SD (n=3, $^{**}p<0.01$). **(F)** The growth curve of ARP-1 cells transfected with shHMGB1. ARP-1 cells were transiently transfected with scramble or HMGB1 specific shRNA and cultured with a density of 1×10^5 cells/ml. Total number of Trypan Blue negative cells were manually counted at the indicated time points and plotted ($^{**}p<0.01$). **(G)** ARP-1 cells were transiently transfected with a vector encoding HMGB1 (ovHMGB1) or a blank (Mock) vector for different time and subjected to a CCK-8 assay. Data are presented from three independent experiments as the mean±SD ($^{*}p<0.05$). **(H)** ARP-1 cells were transiently transfected with Mock or ovHMGB1 vector, cultured and counted as indicated in F and growth curve was generated ($^{*}p<0.05$).

Lycorine mediated proteasomal degradation of HMGB1 inhibits the dissociation of Bcl-2 from Beclin-1

We further explored the mechanisms leading to the down-regulation of HMGB1 protein upon lycorine treatment. Both intracellular and extracellular HMGB1 are critical in regulating autophagy [20]. No release of HMGB1 was detected outside of the cells after lycorine treatment in both ANBL6 and ARP-1 cells (Figure 4A). We then examined whether lycorine has effects on HMGB1 location by immunoflourescent staining and Western blotting analysis of the cytoplasmic and nuclear fractions from the control and lycorine-treated ANBL6 and ARP-1 cells. Lycorine treatment resulted in a remarkable decrease of HMGB1 protein both in the cytoplasm and in the nucleus (Figure 4B and C). These results indicated that lycorine affects HMGB1 pool inside the cell. Quantitative RT-PCR showed that HMGB1 mRNA level was not decreased in cells after lycorine treatment (Figure 4D). However, a reduction of the HMGB1 protein levels was observed by Western blotting (Figure 2B). This suggested that lycorine downregulated HMGB1 expression at the post-translational level. The effect of lycorine on HMGB1 protein stability was then analyzed using Cycloheximide (CHX) chase. Lycorine treatment caused an accelerated degradation of HMGB1 protein compared to control group treated with CHX alone (Figure 4E). Furthermore, the proteasome inhibitor MG-132 was applied to investigate whether HMGB1 undergoes degradation via a proteasome pathway. Lycorine-mediated decrease in HMGB1 protein levels in ANBL6 cells were nearly completely prevented in the presence of MG-132 (Figure 4F). Quantitative Co-IP accomplished that ubiquitinated HMGB1 accumulated upon lycorine treatment (Figure 4G) confirming lycorine enhanced the degradation of HMGB1 by the ubiquitin-proteasome pathway. We investigated the mechanism of lycorine mediated HMGB1 degradation and autophagy inhibition. It was shown that HMGB1 promotes autophagy initiation through the transcriptional activation of MEK-ERK and subsequent dissociation of Bcl-2 as p-Bcl-2 from Beclin-1 [13, 36, 37]. Lycorine markedly diminished the phosphorylation of MEK, ERK1/2 and Bcl-2 (Figure 4H). Furthermore, increased amount of Bcl-2 was co-immunoprecipitated with Beclin-1 confirming the inhibition of Bcl-2 dissociation from Beclin-1 (Figure 4I). These findings indicated that, proteasomal degradation of HMGB1 by lycorine inactivates MEK-ERK pathway. This results in inhibition of Bcl-2 dissociation from Beclin-1, consequently autophagy inhibition.

Lycorine enhances the effect of BTZ by inhibiting autophagy

Bortezomib (BTZ) is commonly used in the systematic treatment of MM. To examine whether lycorine enhances the inhibitory effect of BTZ, MM cells were cultured for 24 h with 15 nM BTZ in the presence or absence of 10 μM lycorine. A CCK-8 assay indicated that lycorine enhances the growth inhibition mediated by BTZ (Figure 5A). Furthermore, combination of additional concentrations of lycorine and BTZ were tested and calculations of combination index (CI) values using CompuSyn software indicated synergistic effects between lycorine and BTZ in vitro (Figure 5B). Recent studies suggested that BTZ induced autophagy is responsible for acquired resistance against this drug [38-41]. Next, we aimed to investigate the effect of lycorine-BTZ combination on autophagy. Interestingly, treatment with lycorine not only enhanced the efficacy of BTZ but also significantly decreased BTZ-induced autophagy, as confirmed by analyzing LC3B and Beclin-1 expression in both MM cell lines (Figure 5C). In a time based experiment we found that the simultaneous exposure of lycorine and BTZ from 0 to 18 h cannot induce HMGB1 down regulation as well as autophagy inhibition. Albeit, prolong period of simultaneous incubation from 21 to 24 h caused decrease of HMGB1 level with a concomitant inhibition of autophagy (Supplementary Figure S2). Concerning the importance of bone marrow microenvironment in MM progression [42, 43], the effect of lycorine on MM cell growth in the presence of BMSCs was examined. The results showed that lycorine had no effect on the BMSC cell line HS5 (Supplementary Figure S3). However, ANBL6 and ARP-1 cells co-cultured with HS5 cells and treated with lycorine, BTZ or a combination of both exhibited a significant decrease in cell viability, and the combined effect of lycorine plus BTZ was higher than individual treatments with either compound (Figure 5D). For all combinations of treatments in the BM microenvironment, lycorine was found to enhance the activity of BTZ (Supplementary Figure S4). Importantly, lycorine also significantly decreased the viability and enhanced BTZ activity against $CD138^+$ primary MM cells from patients. It is worth noting that lycorine at a concentration that inhibits patient primary cell viability does not significantly affect the viability of primary $CD138^+$ cells from normal healthy donor (Figure 5E). HMGB1 promotes drug resistance in different tumors. We therefore examined whether HMGB1 expression reflects a pro-survival effect in bortezomib resistance ANBL6.BR cells. We observed higher level of HMGB1 expression in ANBL6.BR cells compared to bortezomib naïve ANBL6.WT cells (Figure 5F).

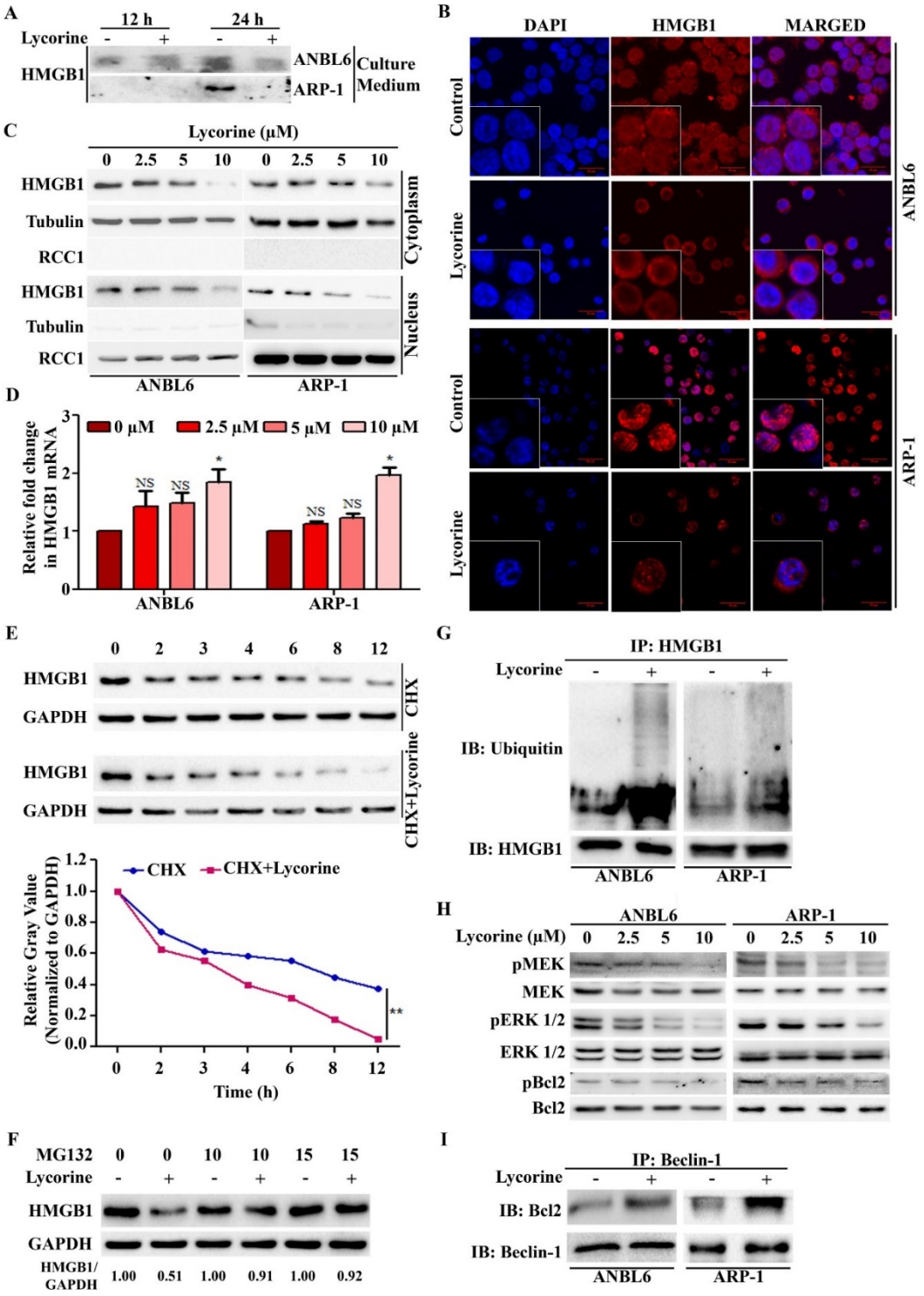

Figure 4. Lycorine mediated proteasomal degradation of HMGB1 inhibits the dissociation of Bcl-2 from Beclin-1. (A) Release of HMGB1 upon lycorine treatment was analyzed. The amount of HMGB1 was checked in the culture medium of ANBL6 and ARP-1 cells after incubation with or without lycorine for 12 and 24 h by Western blotting. (**B**) Subcellular localization of HMGB1 was observed under confocal microscope. ANBL6 and ARP-1 cells were treated with or without lycorine for 24 h and then immunostained with HMGB1-specific antibody/Cy3 secondary antibody (shown in red). Nuclei were stained with DAPI (blue). Images were acquired digitally by FV1000-X81 confocal microscope (Olympus, Japan) with 60× magnification. **(C)** Subcellular localization of HMGB1 was checked by Western blotting. Cytoplasmic and nuclear extracts of the harvested ANBL6 and ARP-1 cells after 24 h treatment with increasing doses of lycorine were prepared and subjected to Western blotting for the detection of HMGB1. Antibodies against α-tubulin and RCC1 were used to determine the purity of the cytoplasmic and nuclear fractions, respectively. **(D)** Total RNA was prepared from ANBL6 and ARP-1 cells 24 h after lycorine treatment and the level of HMGB1 mRNA was measured by quantitative RT-PCR. **(E)** Western blotting analysis of total cell lysate prepared from cells treated with 200 μg/ml CHX in the presence or absence of lycorine for the indicated time. The signal intensity from HMGB1 blot was normalized to GAPDH and plotted against the CHX incubation time. **(F)** Cells were incubated for 18 h with or without lycorine, followed by 6 h with 10 or 15 μM MG-132, and the lysate was used to detect HMGB1. GAPDH was used as a loading control. Densitometry analysis of HMGB1 intensity was performed using ImageJ software and normalized with loading control (HMGB1/GAPDH). **(G)** Quantitative Co-IP was adopted to investigate the interaction of HMGB1 with ubiquitin. Co-IP was performed using an anti-HMGB1 antibody in lysate from cells treated with or without lycorine and subjected for Western blotting. The blot was then probed with an anti-ubiquitin antibody. **(H)** Effect of different concentration of lycorine on MEK-ERK pathway. Total protein lysates were analyzed by immunoblotting using the indicated antibodies. Levels of total MEK, ERK 1/2 and Bcl2 were normalized for equal loading to detect their activated phosphorylation state. **(I)** Association of Bcl-2 with Beclin-1 was analyzed by Quantitative Co-IP. After immunoprecipitation using Beclin-1 antibody, sample was blotted and probed with Bcl-2 antibody.

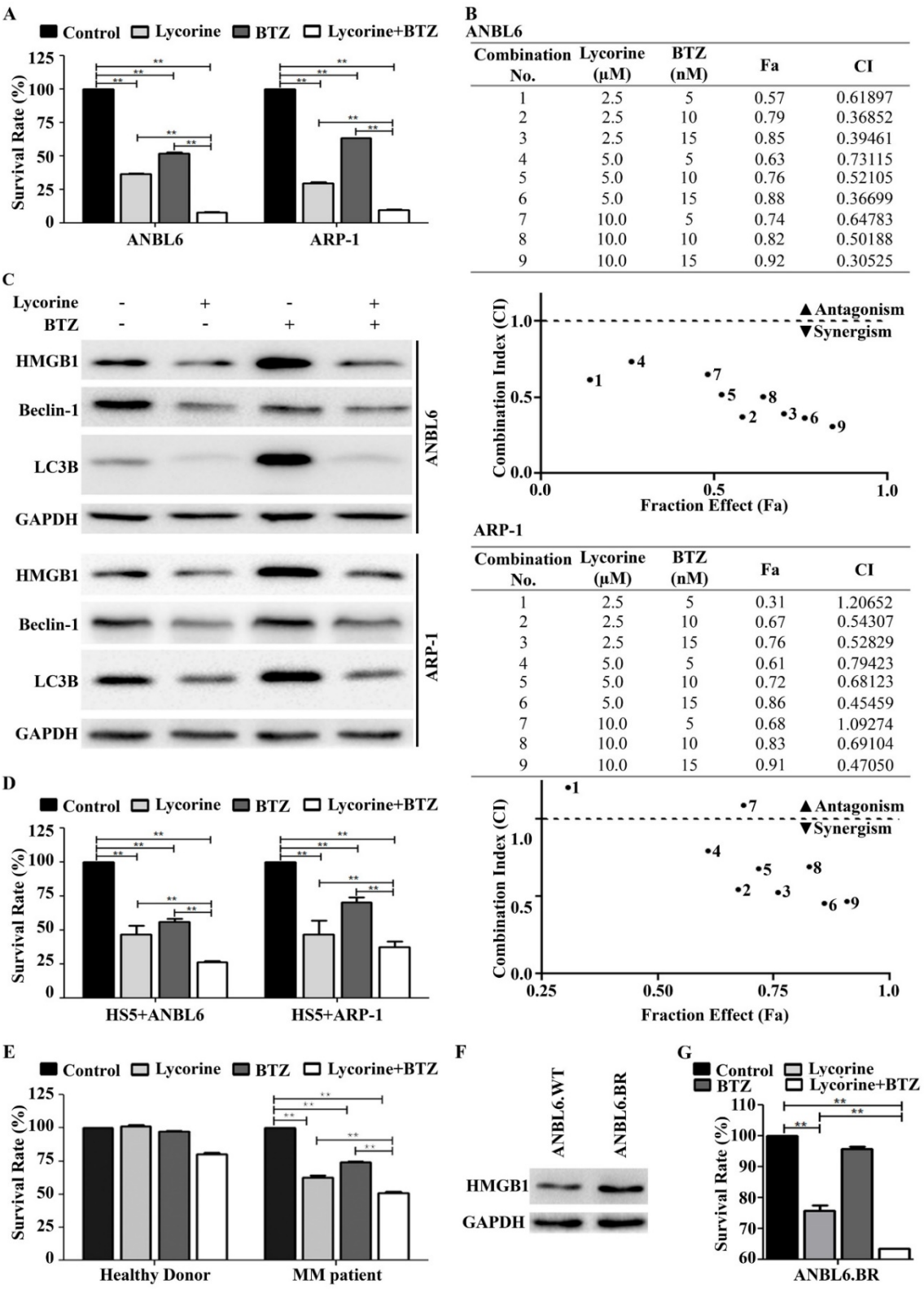

Figure 5. Lycorine enhances the effect of bortezomib by inhibiting autophagy. (A) ANBL6 and ARP-1 cells were grown and treated with lycorine, BTZ or lycorine plus BTZ, then cell viability was obtained using a CCK-8 assay. Data are presented as the mean±SD (n=3, $^{**}p<0.01$). **(B)** Combination index of lycorine and BTZ. ANBL6 and ARP-1 cells were treated 24 h across a range of concentrations of lycorine, BTZ or lycorine plus BTZ, and assessed for cell viability using CCK-8 assay. Combination index (CI) values corresponding to the specified data points on the table were obtained using CompuSyn software program for non-constant drug ratio and plotted on the graph against fraction effect (Fa) to detect lycorine-BTZ synergy. A CI<1 indicates synergism **(C)** After ANBL6 and ARP-1 cells were treated with lycorine, BTZ or lycorine plus BTZ, the expression of HMGB1 and the autophagy-related proteins Beclin-1 and LC3B was analyzed by Western blotting. GAPDH was used as a loading control. **(D)** Activity of lycorine against ANBL6 and ARP-1 cells in the presence of bone marrow stromal cells (BMSC) was analyzed by cell viability assay using a CCK-8 kit. Data presented are mean±SD (n=3, $^{**}p<0.01$). **(E)** Effect of lycorine on primary bone marrow cells. Human primary BM CD138$^+$ cells were treated with lycorine, BTZ and lycorine plus BTZ for 24 h and cell viability was measured by CCK-8 assay. Data presented are mean±SD from triplicate samples ($^{**}p<0.01$). **(F)** Western blotting analysis of basal HMGB1 expression in bortezomib-naïve and bortezomib-resistance ANBL6 cells. **(G)** Effect of lycorine, BTZ and combination on BTZ resistance ANBL6.BR cells was analyzed by cell viability assay. Data were generated from three independent experiments ($^{**}p<0.01$).

We further investigated the functional effect of combined lycorine and BTZ in ANBL6.BR cells. Lycorine treatment alone can reduced cell viability in ANBL6.BR and combined with BTZ exposure, the effect was enhanced significantly (Figure 5G).

Lycorine attenuates tumor growth in vivo in MM xenograft mouse model by inhibiting autophagy

Having shown the potential anti-myeloma effect in vitro, we next examined the therapeutic effects of lycorine and BTZ combination treatment in vivo using a MM xenograft NOD/SCID mouse model. BTZ and Lycorine were given by intraperitoneal injection at the time the tumor could be palpated under the skin (at day14 after MM cells injection). Tumor growth patterns in mice showed that lycorine treatment efficiently inhibit tumor growth from day 18 to day 26 (Figure 6A). Tumor size was significantly decreased after treatment with lycorine (1756±728 mm^3) or BTZ (1981±402 mm^3) compared with control (3381±468 mm^3) (Figure 6B) at day 26. Notably, the volumes of tumors were much lower in the group treated with BTZ in combination with lycorine (895±643 mm^3) (Figure 6A and B) at day 26. During the treatment period, no significant change in body weight was observed (Figure 6C), indicating no evidence of toxicity caused by the applied doses of lycorine and combination. HE staining revealed a relatively low density of tumor cells and a much higher density of necrotic cells in lycorine-treated xenograft tumor sections compared to the densities in the control group. Increased numbers of apoptotic tumor cells were also detected by TdT-mediated dUTP nick-end labeling (TUNEL) assay in mice treated with lycorine compared with that of untreated group (Figure 6D).

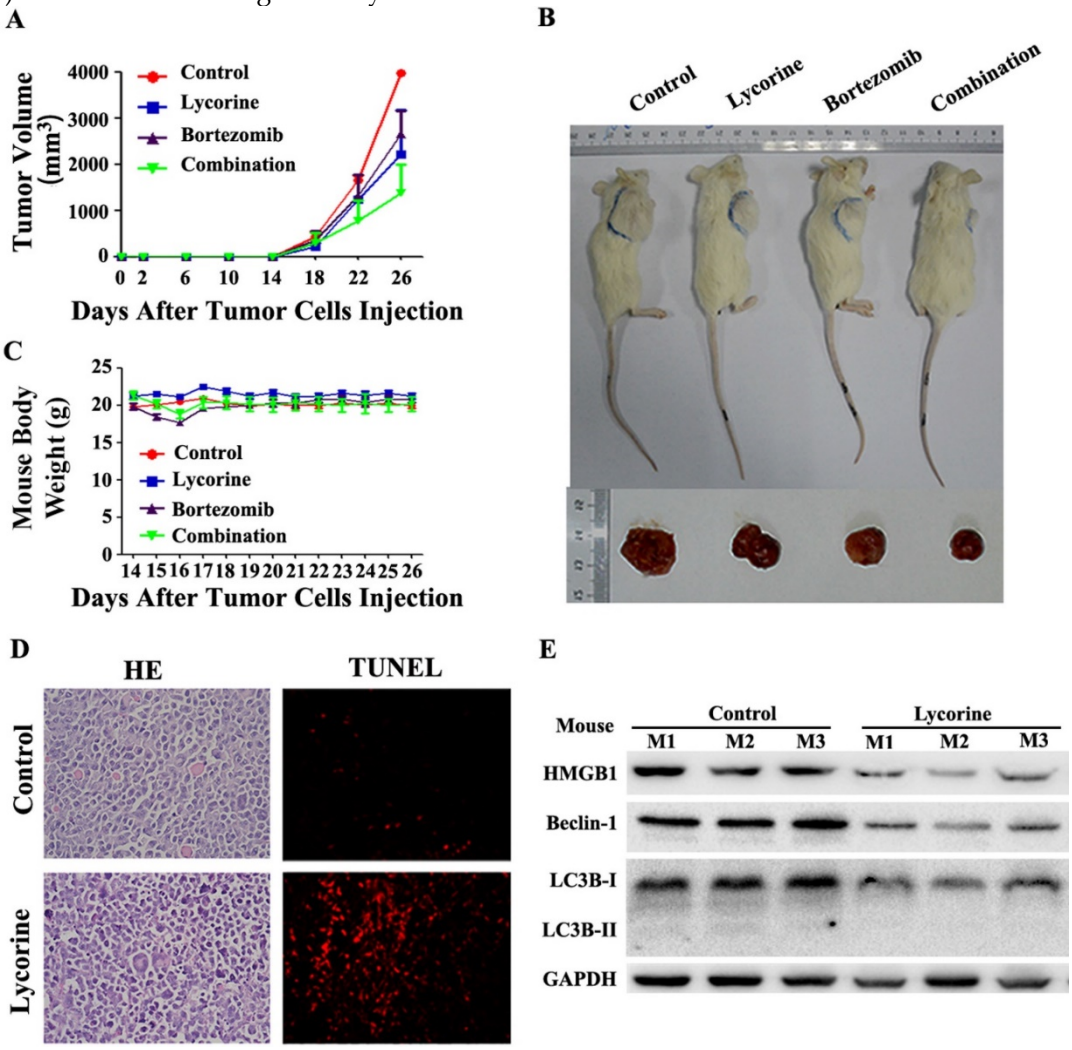

Figure 6. Anti-MM activity of lycorine in MM xenograft mouse models. (A) Changes in tumor volume. Caliper measurement of the tumor diameters were performed very 4 days to estimate the tumor volume using the following formula ($a \times b^2$)/2, where 'a' and 'b' respectively are the longest and shortest perpendicular diameters of tumor. Data are presented as the mean±SD from five mice. **(B)** Representative tumor bearing mouse from each treatment group before dissection (top). The mice were euthanized at the treatment end point, tumors were removed and photographed (bottom). **(C)** During the treatment period, mouse body weight was measured every 4 days. Data are shown as mean±SD. **(D)** Histochemical examinations of mouse tissue section. Tissue sections from the tumor were fixed and stained with HE and TUNEL to examine the tumor cell morphology. The magnifications are 40×. **(E)** Western blotting analysis of the expression of HMGB1, Beclin-1 and LC3B in lysate extracted from tumor tissues. GAPDH was used as a loading control.

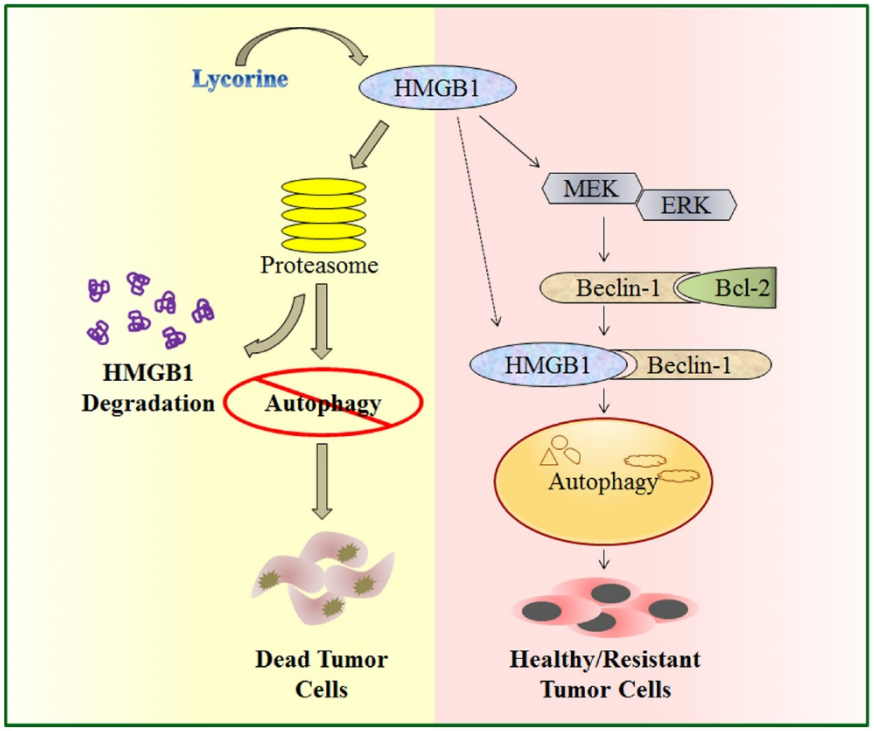

Figure 7. A schematic illustration of proposed mechanism for anti-myeloma activity of lycorine. HMGB1 acts as an important mediator of autophagy. It can directly bind with Beclin-1 or activate MEK-ERK to free Beclin-1 from Bcl-2 and initiate autophagy which facilitates cell survival and confers resistance. Lycorine is suggested to mediate HMGB1 degradation through proteasome pathway, inhibits MEK-ERK activation and thereby increase Bcl-2-Beclin-1 interaction. As a result causes inhibition of pro-survival autophagy and leads to cell death.

Moreover, Western blotting analysis of proteins extracted from the xenograft showed that the expression of LC3B, Beclin-1 and HMGB1 had been downregulated in the lycorine-treated group (Figure 6E), but the mRNA level of HMGB1 did not significantly change (Supplementary Figure S5). These results demonstrated the efficacy of lycorine in inhibiting in vivo tumor growth by decreasing HMGB1 protein and thereby inhibiting autophagy and enhancing BTZ effect.

Discussion

In the present study, we explored the function and underlying mechanisms of anti-MM effects of lycorine. We demonstrated that by activating the proteasomal degradation of HMGB1, lycorine induces a rapid turnover of HMGB1. This led to decreased Bcl-2 phosphorylation by MEK-ERK pathway and increased association of Bcl-2 with Beclin-1 resulting in autophagy inhibition and growth attenuation (Figure 7). This is the first report demonstrating a model to show the critical role of HMGB1 in MM cell survival and bortezomib (BTZ) resistance which could be overcome by lycorine.

In the era of new and most effective therapies for MM, the proteasome inhibitor BTZ and the immunomodulatory drugs thalidomide and lenalidomide, in particular, have rapidly improved MM therapy and patient outcomes [44]. However, the current clinical issues are drug resistance and relapse because of the heterogeneous genetic/epigenetic basis of the disease as well as noncoding regulatory RNA such as microRNA (miRNAs) and the bone marrow microenvironment components [45-47]. Ongoing studies aim to develop personalized therapies, immune-based therapies, next-generation targeted agents, and rationally based combinations of targeted therapies [4, 47]. Considering the anti-proliferative activity, lycorine can be a lead compound for new drug design to treat cancer. In this study, lycorine showed selective inhibitory effects against MM cell lines regardless of genetic background and in vivo myeloma xenograft model.

Autophagy, a process for recycling cellular constituents, is associated with cell survival and tumor maintenance [48, 49]. Plasma cells heavily rely on autophagy during the differentiation of B-cells and maintenance of antibody secretion [35, 50, 51]. Hence, inhibiting autophagy may be beneficial against MM cells. We have previously found that the anti-MM effect of lycorine is associated with cell cycle arrest in G1 phase, increased reactive oxygen species (ROS) generation and DNA damage resulted from accumulation of dysfunctional mitochondria [29]. Mitochondria are the key targets for autophagy [52, 53]. Furthermore, autophagy acts as a driving force

for cell cycle entry via the upregulation of cyclin D, an essential regulator of the progression through G1 in response to mitogenic signals [54]. Autophagy also permits DNA replication, and thereby promotes cell cycle progression and cell proliferation [55]. In our present study, the natural compound lycorine was shown to inhibit autophagy in MM. Combined with our previous study imply that the main effect of lycorine may through the inhibition of autophagy. Combining 3-MA with lycorine did not enhance the growth inhibition efficiency of lycorine, suggesting that the molecular target of lycorine may converge upon the same pathway with that of 3-MA and also indicates autophagy inhibition as an important contributor of lycorine induced anti-MM activity.

HMGB1 is an important mediator of autophagy and HMGB1-mediated autophagy is responsible for the inhibition of apoptosis and the induction of drug resistance [56, 57]. Our results indicated HMGB1 as a key mediator of lycorine-induced autophagy inhibition and thereby proliferation attenuation. The association of HMGB1 with the development of cancer is evident [20]. HMGB1 expression regulates chemotherapeutic responses and resistance by interfering with autophagy and the apoptotic pathway. These traits make HMGB1 a novel target for anti-cancer therapy [58]. NEK2, a chromosomal instability (CIN) gene has been defined previously to be highly correlated with drug resistance, rapid relapse, and poor outcomes in MM, was immensely related to HMGB1 in the GEP analysis [59]. GEP analysis of the public accession database in our study, for the first time indicated that higher expression of HMGB1 is linked with the poor prognosis of MM. This observation was further confirmed by the finding of higher HMGB1 expression in myeloma cell lines and in patient primary $CD138^+$ cells. Furthermore, our result showed that, HMGB1 overexpression and knockdown could enhance or decline cell growth and proliferation respectively in vitro, indicating HMGB1 is involved in the pathogenesis of MM and can be a potential therapeutic target for the treatment of MM.

Searching for the mechanisms underlying the role of lycorine in downregulating HMGB1, we found that lycorine decrease HMGB1 pool inside the cell. Downregulation of HMGB1 by lycorine occurs at post-translational level and mediated through the ubiquitin proteasome pathway. Although it has been clarified that HMGB1 can be degraded by ubiquitin-proteasome pathway after lycorine treatment, the E3 ligases for HMGB1 are so far unclear and need further exploration. Interaction of Beclin-1 with several cofactors holds a central role for regulating autophagy [60, 61]. Release of Bcl-2 as phosphorylated Bcl-2, from Beclin-1 results in the formation of Beclin-1-PI3K autophagosome nucleation complex. HMGB1 mediated activation of MEK-ERK1/2 regulates the phosphorylation of Bcl-2 and autophagy [62, 63]. Our observations that degradation of HMGB1 by lycorine inhibits the phosphorylation of MEK-ERK1/2 and inhibits the dissociation of Bcl-2 from Beclin-1 also supported these findings. This is why PI3K inhibitor 3-MA has no additive effect on lycorine-induced cell death related to autophagy. Endogenous HMGB1 can interfere the interaction between Beclin-1 and Bcl-2 to regulate autophagy [63]. We found lycorine can diminish the protein level of HMGB1 and blocks the dissociation of Bcl-2 from Beclin-1 to inhibit autophagy.

To improve response rates and prolong response duration, new therapeutics combinations with BTZ and other anti-MM agents has been frequently used in preclinical studies [64, 65]. In the present study, we determined that the combination of lycorine and BTZ was more effective in vitro, primary patient $CD138^+$ cells and in vivo than either agent alone. Moreover, recent studies demonstrated that, BTZ induced autophagy results in drug resistance [39-41]. Interestingly, in our study, the combination of lycorine and BTZ significantly reduced BTZ-induced autophagy. We found that the proteasome inhibitor BTZ prevents HMGB1 degradation and autophagy inhibition in a 0 to 18 h frame of combine treatment. However, 21 to 24 h combine treatment increases HMGB1 degradation and autophagy inhibition presumably because at that time point lycorine dominates over BTZ activity. Therefore, it is suggestive that the combine effect of lycorine and BTZ is related to timing and synchronizing the doses of these two drugs can be synergistic to induce myeloma cell death. Yet the detail mechanism demands further investigation. By utilizing an in vitro model of BTZ resistant MM, we found a higher basal level of HMGB1 protein in bortezomib-resistant MM cell line and a failure of these cells to respond to bortezomib. Lycorine treatment restored a measurable cytotoxic response to BTZ in BTZ resistant MM cell, reflecting the potential of lycorine to overcome BTZ resistance.

In conclusion, our results elucidated that lycorine, as a single agent, is active against MM. This study provides proof-of-principle for further exploring the role of HMGB1 and the potential clinical application of lycorine in MM treatment. At the same time it suggests a preclinical framework for combining lycorine and BTZ in clinical settings. Considering the high capability of lycorine combating cancers, our present study including other previously reported studies offers synthetic organic chemists some rational to investigate the chemistry associated

with this alkaloid, its active moiety such as phenolic and alcoholic groups, the insaturation pattern, and the presence of amine group to make this compound more therapeutically achievable and lower toxic.

Acknowledgments

This work was supported by the grants from the National Natural Science Foundation of China (81470362, 30971517, 81600184, 81301774, 81400169, 81272220 and 81171950), Postgraduate innovation project of Central South University of China (CX2014B101, 2016zzts165 and 2016zzts582) and the Program for New Century Excellent Talents in University (NCET-13-0195).

Authorship Contributions

M.R, L.L, X.X and Y.P contributed equally to this work. J.L, W.Z, M.Y, L.Q and F.L designed the research, J.L, M.R, L.L, M.Y and W.Z organized, analyzed, and interpreted the data; M.R, L.L, X.X, Y.P, Y.L, W.Z, J.Z and S.Z performed the experiments; M.R, W.Z and J.L drafted and revised the manuscript.

Supplementary Material

Supplementary figures.
http://www.thno.org/v06p2209s1.pdf

Competing Interests

The authors have declared that no competing interest exists.

References

1. Rollig C, Knop S, Bornhauser M. Multiple myeloma. Lancet. 2015; 385: 2197-208.
2. Fonseca R, Bergsagel PL, Drach J, Shaughnessy J, Gutierrez N, Stewart AK, et al. International Myeloma Working Group molecular classification of multiple myeloma: spotlight review. Leukemia. 2009; 23: 2210-21.
3. Corre J, Munshi N, Avet-Loiseau H. Genetics of multiple myeloma: another heterogeneity level? Blood. 2015; 125: 1870-6.
4. Licht JD, Shortt J, Johnstone R. From anecdote to targeted therapy: the curious case of thalidomide in multiple myeloma. Cancer Cell. 2014; 25: 9-11.
5. Choi AM, Ryter SW, Levine B. Autophagy in human health and disease. N Engl J Med. 2013; 368: 651-62.
6. White E. Deconvoluting the context-dependent role for autophagy in cancer. Nat Rev Cancer. 2012; 12: 401-10.
7. Kawaguchi T, Miyazawa K, Moriya S, Ohtomo T, Che XF, Naito M, et al. Combined treatment with bortezomib plus bafilomycin A1 enhances the cytocidal effect and induces endoplasmic reticulum stress in U266 myeloma cells: crosstalk among proteasome, autophagy-lysosome and ER stress. Int J Oncol. 2011; 38: 643-54.
8. Zhao S, Ma CM, Liu CX, Wei W, Sun Y, Yan H, et al. Autophagy inhibition enhances isobavachalcone-induced cell death in multiple myeloma cells. Int J Mol Med. 2012; 30: 939-44.
9. Zhang H, Chen J, Zeng Z, Que W, Zhou L. Knockdown of DEPTOR induces apoptosis, increases chemosensitivity to doxorubicin and suppresses autophagy in RPMI-8226 human multiple myeloma cells in vitro. Int J Mol Med. 2013; 31: 1127-34.
10. Vogl DT, Stadtmauer EA, Tan KS, Heitjan DF, Davis LE, Pontiggia L, et al. Combined autophagy and proteasome inhibition: a phase 1 trial of hydroxychloroquine and bortezomib in patients with relapsed/refractory myeloma. Autophagy. 2014; 10: 1380-90.
11. Mishima Y, Santo L, Eda H, Cirstea D, Nemani N, Yee AJ, et al. Ricolinostat (ACY-1215) induced inhibition of aggresome formation accelerates carfilzomib-induced multiple myeloma cell death. Br J Haematol. 2015; 169: 423-34.
12. Carew JS, Kelly KR, Nawrocki ST. Autophagy as a target for cancer therapy: new developments. Cancer Manag Res. 2012; 4: 357-65.
13. Tang D, Kang R, Livesey KM, Cheh CW, Farkas A, Loughran P, et al. Endogenous HMGB1 regulates autophagy. J Cell Biol. 2010; 190: 881-92.
14. Tang D, Kang R, Livesey KM, Kroemer G, Billiar TR, Van Houten B, et al. High-mobility group box 1 is essential for mitochondrial quality control. Cell Metab. 2011; 13: 701-11.
15. Huang J, Ni J, Liu K, Yu Y, Xie M, Kang R, et al. HMGB1 promotes drug resistance in osteosarcoma. Cancer Res. 2012; 72: 230-8.
16. Goodwin GH, Sanders C, Johns EW. A new group of chromatin-associated proteins with a high content of acidic and basic amino acids. Eur J Biochem. 1973; 38: 14-9.
17. Ellerman JE, Brown CK, de Vera M, Zeh HJ, Billiar T, Rubartelli A, et al. Masquerader: high mobility group box-1 and cancer. Clin Cancer Res. 2007; 13: 2836-48.
18. Tang D, Kang R, Zeh HJ, 3rd, Lotze MT. High-mobility group box 1 and cancer. Biochim Biophys Acta. 2010; 1799: 131-40.
19. Liu L, Yang M, Kang R, Wang Z, Zhao Y, Yu Y, et al. HMGB1-induced autophagy promotes chemotherapy resistance in leukemia cells. Leukemia. 2011; 25: 23-31.
20. Kang R, Zhang Q, Zeh HJ, 3rd, Lotze MT, Tang D. HMGB1 in cancer: good, bad, or both? Clin Cancer Res. 2013; 19: 4046-57.
21. Balunas MJ, Kinghorn AD. Drug discovery from medicinal plants. Life Sci. 2005; 78: 431-41.
22. Shanmugam MK, Lee JH, Chai EZ, Kanchi MM, Kar S, Arfuso F, et al. Cancer prevention and therapy through the modulation of transcription factors by bioactive natural compounds. Semin Cancer Biol. 2016.
23. Cragg GM, Newman DJ. Plants as a source of anti-cancer agents. J Ethnopharmacol. 2005; 100: 72-9.
24. Newman DJ, Cragg GM. Natural products as sources of new drugs over the 30 years from 1981 to 2010. J Nat Prod. 2012; 75: 311-35.
25. Liu J, Hu WX, He LF, Ye M, Li Y. Effects of lycorine on HL-60 cells via arresting cell cycle and inducing apoptosis. FEBS Lett. 2004; 578: 245-50.
26. Liu J, Li Y, Tang LJ, Zhang GP, Hu WX. Treatment of lycorine on SCID mice model with human APL cells. Biomed Pharmacother. 2007; 61: 229-34.
27. Li Y, Liu J, Tang LJ, Shi YW, Ren W, Hu WX. Apoptosis induced by lycorine in KM3 cells is associated with the G0/G1 cell cycle arrest. Oncol Rep. 2007; 17: 377-84.
28. Liu XS, Jiang J, Jiao XY, Wu YE, Lin JH, Cai YM. Lycorine induces apoptosis and down-regulation of Mcl-1 in human leukemia cells. Cancer Lett. 2009; 274: 16-24.
29. Luo Y, Roy M, Xiao X, Sun S, Liang L, Chen H, et al. Lycorine induces programmed necrosis in the multiple myeloma cell line ARH-77. Tumour Biol. 2015; 36: 2937-45.
30. Lamoral-Theys D, Andolfi A, Van Goietsenoven G, Cimmino A, Le Calve B, Wauthoz N, et al. Lycorine, the main phenanthridine Amaryllidaceae alkaloid, exhibits significant antitumor activity in cancer cells that display resistance to proapoptotic stimuli: an investigation of structure-activity relationship and mechanistic insight. J Med Chem. 2009; 52: 6244-56.
31. Hu M, Peng S, He Y, Qin M, Cong X, Xing Y, et al. Lycorine is a novel inhibitor of the growth and metastasis of hormone-refractory prostate cancer. Oncotarget. 2015; 6: 15348-61.
32. Dasari R, Banuls LM, Masi M, Pelly SC, Mathieu V, Green IR, et al. C1,C2-ether derivatives of the Amaryllidaceae alkaloid lycorine: retention of activity of highly lipophilic analogues against cancer cells. Bioorg Med Chem Lett. 2014; 24: 923-7.
33. Chou TC. Theoretical basis, experimental design, and computerized simulation of synergism and antagonism in drug combination studies. Pharmacol Rev. 2006; 58: 621-81.
34. Shi Y, Han Y, Xie F, Wang A, Feng X, Li N, et al. ASPP2 enhances oxaliplatin (L-OHP)-induced colorectal cancer cell apoptosis in a p53-independent manner by inhibiting cell autophagy. J Cell Mol Med. 2015; 19: 535-43.
35. Carroll RG, Martin SJ. Autophagy in multiple myeloma: what makes you stronger can also kill you. Cancer Cell. 2013; 23: 425-6.
36. Pan B, Chen D, Huang J, Wang R, Feng B, Song H, et al. HMGB1-mediated autophagy promotes docetaxel resistance in human lung adenocarcinoma. Mol Cancer. 2014; 13: 165.
37. Liu W, Zhang Z, Zhang Y, Chen X, Guo S, Lei Y, et al. HMGB1-mediated autophagy modulates sensitivity of colorectal cancer cells to oxaliplatin via MEK/ERK signaling pathway. Cancer Biol Ther. 2015; 16: 511-7.
38. Milan E, Perini T, Resnati M, Orfanelli U, Oliva L, Raimondi A, et al. A plastic SQSTM1/p62-dependent autophagic reserve maintains proteostasis and determines proteasome inhibitor susceptibility in multiple myeloma cells. Autophagy. 2015; 11: 1161-78.
39. Escalante AM, McGrath RT, Karolak MR, Dorr RT, Lynch RM, Landowski TH. Preventing the autophagic survival response by inhibition of calpain enhances the cytotoxic activity of bortezomib in vitro and in vivo. Cancer Chemother Pharmacol. 2013; 71: 1567-76.
40. Zhang M, He J, Liu Z, Lu Y, Zheng Y, Li H, et al. Anti-beta(2)-microglobulin monoclonal antibodies overcome bortezomib resistance in multiple myeloma by inhibiting autophagy. Oncotarget. 2015; 6: 8567-78.
41. Jagannathan S, Abdel-Malek MA, Malek E, Vad N, Latif T, Anderson KC, et al. Pharmacologic screens reveal metformin that suppresses GRP78-dependent autophagy to enhance the anti-myeloma effect of bortezomib. Leukemia. 2015; 29: 2184-91.

42. Uchiyama H, Barut BA, Mohrbacher AF, Chauhan D, Anderson KC. Adhesion of human myeloma-derived cell lines to bone marrow stromal cells stimulates interleukin-6 secretion. Blood. 1993; 82: 3712-20.
43. Kawano Y, Moschetta M, Manier S, Glavey S, Gorgun GT, Roccaro AM, et al. Targeting the bone marrow microenvironment in multiple myeloma. Immunol Rev. 2015; 263: 160-72.
44. Moreau P, Attal M, Facon T. Frontline therapy of multiple myeloma. Blood. 2015; 125: 3076-84.
45. Abdi J, Chen G, Chang H. Drug resistance in multiple myeloma: latest findings and new concepts on molecular mechanisms. Oncotarget. 2013; 4: 2186-207.
46. Zhang J, Xiao X, Liu J. The role of circulating miRNAs in multiple myeloma. Sci China Life Sci. 2015; 58: 1262-9.
47. Anderson KC. New insights into therapeutic targets in myeloma. Hematology Am Soc Hematol Educ Program. 2011; 2011: 184-90.
48. Chen P, Cescon M, Bonaldo P. Autophagy-mediated regulation of macrophages and its applications for cancer. Autophagy. 2014; 10: 192-200.
49. Thorburn A, Thamm DH, Gustafson DL. Autophagy and cancer therapy. Mol Pharmacol. 2014; 85: 830-8.
50. Pengo N, Scolari M, Oliva L, Milan E, Mainoldi F, Raimondi A, et al. Plasma cells require autophagy for sustainable immunoglobulin production. Nat Immunol. 2013; 14: 298-305.
51. Arnold J, Murera D, Arbogast F, Fauny JD, Muller S, Gros F. Autophagy is dispensable for B-cell development but essential for humoral autoimmune responses. Cell Death Differ. 2016; 23: 853-64.
52. Okamoto K, Kondo-Okamoto N. Mitochondria and autophagy: critical interplay between the two homeostats. Biochim Biophys Acta. 2012; 1820: 595-600.
53. Schiavi A, Ventura N. The interplay between mitochondria and autophagy and its role in the aging process. Exp Gerontol. 2014; 56: 147-53.
54. Cao Y, Zhang A, Cai J, Yuan N, Lin W, Liu S, et al. Autophagy regulates the cell cycle of murine HSPCs in a nutrient-dependent manner. Exp Hematol. 2015; 43: 229-42.
55. Hubbi ME, Gilkes DM, Hu H, Kshitiz, Ahmed I, Semenza GL. Cyclin-dependent kinases regulate lysosomal degradation of hypoxia-inducible factor 1alpha to promote cell-cycle progression. Proc Natl Acad Sci U S A. 2014; 111: E3325-34.
56. Kang R, Tang D, Schapiro NE, Livesey KM, Farkas A, Loughran P, et al. The receptor for advanced glycation end products (RAGE) sustains autophagy and limits apoptosis, promoting pancreatic tumor cell survival. Cell Death Differ. 2010; 17: 666-76.
57. Huang J, Liu K, Yu Y, Xie M, Kang R, Vernon P, et al. Targeting HMGB1-mediated autophagy as a novel therapeutic strategy for osteosarcoma. Autophagy. 2012; 8: 275-7.
58. Livesey KM, Kang R, Vernon P, Buchser W, Loughran P, Watkins SC, et al. p53/HMGB1 complexes regulate autophagy and apoptosis. Cancer Res. 2012; 72: 1996-2005.
59. Zhou W, Yang Y, Xia J, Wang H, Salama ME, Xiong W, et al. NEK2 induces drug resistance mainly through activation of efflux drug pumps and is associated with poor prognosis in myeloma and other cancers. Cancer Cell. 2013; 23: 48-62.
60. Kang R, Zeh HJ, Lotze MT, Tang D. The Beclin 1 network regulates autophagy and apoptosis. Cell Death Differ. 2011; 18: 571-80.
61. Gordy C, He YW. The crosstalk between autophagy and apoptosis: where does this lead? Protein Cell. 2012; 3: 17-27.
62. He C, Klionsky DJ. Regulation mechanisms and signaling pathways of autophagy. Annu Rev Genet. 2009; 43: 67-93.
63. Kang R, Livesey KM, Zeh HJ, Loze MT, Tang D. HMGB1: a novel Beclin 1-binding protein active in autophagy. Autophagy. 2010; 6: 1209-11.
64. Berenson JR, Yellin O, Kazamel T, Hilger JD, Chen CS, Cartmell A, et al. A phase 2 study of pegylated liposomal doxorubicin, bortezomib, dexamethasone and lenalidomide for patients with relapsed/refractory multiple myeloma. Leukemia. 2012; 26: 1675-80.
65. Berenson JR, Yellin O, Bessudo A, Boccia RV, Noga SJ, Gravenor DS, et al. Phase I/II trial assessing bendamustine plus bortezomib combination therapy for the treatment of patients with relapsed or refractory multiple myeloma. Br J Haematol. 2013; 160: 321-30.